NOAA Technical Memorandum ERL SEL-19

U.S. DEPARTMENT OF COMMERCE
NATIONAL OCEANIC AND ATMOSPHERIC ADMINISTRATION
Environmental Research Laboratories

ARC-1; A Pilot Program of Ionospheric Modification Through Artificial Stimulation of Magnetospherically Trapped Particle Precipitation

DONALD J. WILLIAMS

Space
Environment
Laboratory
BOULDER,
COLORADO
September 1971

ONMENTAL RESEARCH LABORATORIES

SPACE ENVIRONMENT LABORATORY

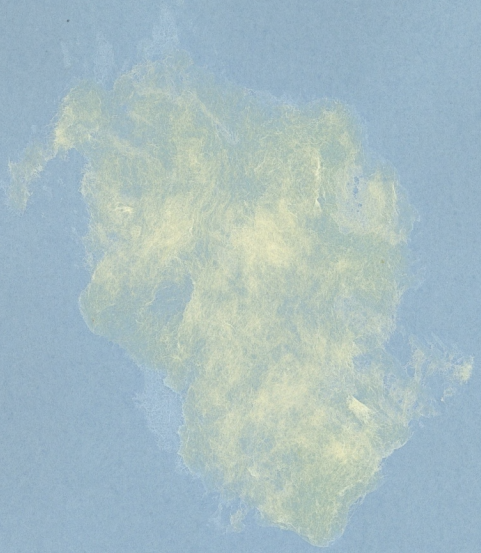

NATIONAL OCEANIC AND ATMOSPHERIC ADMINISTRATION

BOULDER, COLORADO

U.S. DEPARTMENT OF COMMERCE
National Oceanic and Atmospheric Administration
Environmental Research Laboratories

NOAA Technical Memorandum ERL SEL-19

ARC-1; A PILOT PROGRAM OF IONOSPHERIC MODIFICATION THROUGH ARTIFICIAL STIMULATION OF MAGNETOSPHERICALLY TRAPPED PARTICLE PRECIPITATION

Donald J. Williams

Space Environment Laboratory
Boulder, Colorado
September 1971

TABLE OF CONTENTS

ARC-1; A PILOT PROGRAM OF IONOSPHERIC MODIFICATION THROUGH ARTIFICIAL STIMULATION OF MAGNETOSPHERICALLY TRAPPED PARTICLE PRECIPITATION

Donald J. Williams

The injection of cold plasma at geostationary altitudes under favorable ambient environmental conditions can lead to significant energy depositions in the ionosphere through the triggering of a naturally occurring magnetospheric plasma instability, the whistler mode instability. The result of this instability is the scattering of the ambient energetic trapped particle environment down the flux tube into the ionosphere. Nominal energy depositions of $\sim$ 28 ergs/cm^2 sec (2.8 (10^4) microwatts/meter^2) are feasible over a $\sim$ 200 km^2 area in the ionosphere yielding a total energy deposition of $\sim$ 5.6 (10)^6 watts. By contrast visible aurora occur at energy depositions of $\sim$ 1 - 2 ergs/cm^2 sec. These results are discussed along with a pilot satellite program (ARC-1) designed to quantitatively measure cause-effect magnitude over a wide-ranging series of cold plasma injections.

1. INTRODUCTION

The feasibility of even a small measure of control over the energy and energy flow represented by the earth's trapped particle population would give man the use of an enormous energy source ($\sim 10^{15}$ to 10^{16} joules). Because of technical limitations, the control of an energy source this large requires a catalytic mechanism whereby small energy inputs are capable of triggering magnetospheric processes leading to much larger energy flows. Representative of naturally occurring magnetospheric energy flows are energy depositions in the upper atmosphere, ranging from $< 10^{-2}$ ergs cm^{-2}sec^{-1} for moderate 40-keV electron precipitation events, to > 300 ergs cm^{-2}sec^{-1} for large auroral events. Using an area of 10^3km^2 in the lower ionosphere yields a total energy input of from $< 10^4$ watts to > 3 (10)^8 watts for the above examples. Controlled ionospheric heating and ionization are very possible with even small control of such energy flows.

We describe, herein, a satellite program (ARC-1) designed to stimulate the controlled emission of magnetospheric particles into the earth's atmosphere, thereby tapping the source discussed above. The method proposed is to inject cold plasma at geostationary altitudes on the nightside hemisphere in order to trigger a naturally occurring magnetospheric instability, the whistler mode instability. The effect of triggering the whistler mode instability is to scatter the ambient energetic particle population down the geomagnetic field line into the lower ionospheric regions. This is schematically illustrated in figure 1.

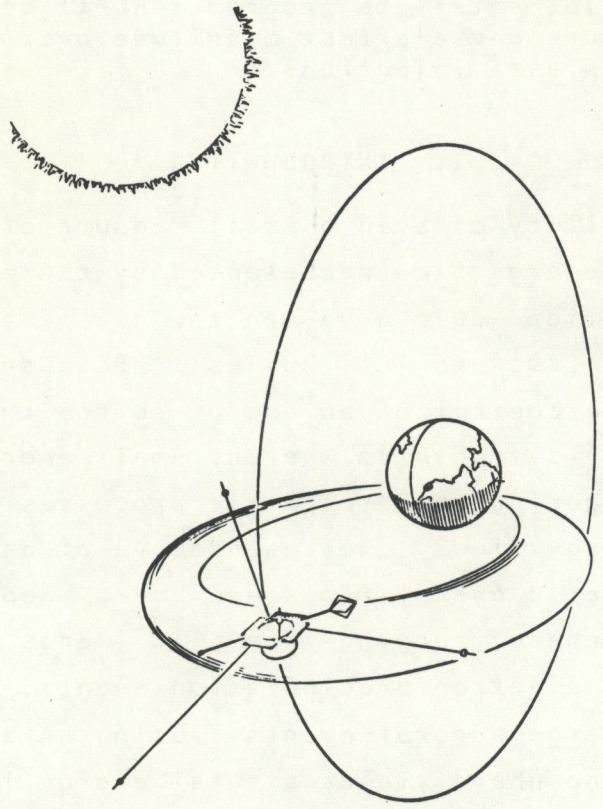

Figure 1. Schematic showing satellite ARC-1 in geostationary orbit. Injection of cold plasma on nightside hemisphere can lead to scattering of ambient trapped energetic particle population down flux tube into ionosphere. Nominal ionospheric energy depositions of tens of ergs/cm^2 sec (> 10^4 microwatts/meter^2) are available.

The initial satellite of the program, ARC-1, will be used to accurately measure cause and effect magnitudes; i.e., the magnitude of the resulting ionospheric disturbances will be quantitatively related to the magnitude of the cold plasma injected at satellite altitude. The resulting ionospheric disturbances will be observed in localized regions above the atmosphere at auroral oval latitudes. Sample calculations indicate that triggering the whistler mode instability with our modest pilot program (ARC-1 weighs approximately 350 pounds) can lead to ionospheric disturbances easily detected by ground instrumentation and possibly even visual aurora.

Details of the material presented in this publication are contained in a four volume study and proposal presented to the ARPA by the Space Environment Laboratory. In developing this report, scientific and technical inputs were gathered not only from the staff of the Space Environment Laboratory (SEL), but also from non-SEL personnel active in magnetospheric research. A Scientific Guidance Committee (SGC) was organized to develop the scientific base and support instrumentation concepts for the mission. This committee met twice, once at the Washington AGU meetings in April 1971, and then at SEL in Boulder during May 1971. The committee members were:

Chairman	D. J. Williams	SEL
	J. R. Cessna	SEL
	D. S. Evans	SEL
	W. Bernstein	SEL
	R. N. Grubb	SEL
	N. Brice	NSF/Cornell
	P. J. Coleman	UCLA
	T. Farley	UCLA
	R. McPherron	UCLA
	J. M. Cornwall	UCLA/Aerospace
	T. N. Davis	University of Alaska
	R. A. Helliwell	Stanford

J. Katsufrakis	Stanford
R. Johnson	Lockheed
F. S. Mozer	University of California at Berkeley
G. A. Paulikas	Aerospace Corporation
J. B. Blake	Aerospace Corporation
M. A. Clark	Aerospace Corporation
M. Shultz	Aerospace Corporation

Additional valuable discussions were held with C. F. Kennel, UCLA, and L. Linson, AVCO, concerning the instability mechanism and its effects. Special acknowledgement is due Dr. J. R. Cessna of SEL who was responsible for defining, assembling, and producing the final report. A brief discussion of the scientific considerations, the satellite system and the expected results follows.

2. SCIENTIFIC CONSIDERATIONS

We shall concentrate on the feasibility of triggering the whistler mode instability (Kennel and Petschek, 1966) through the injection of cold plasma at geostationary altitudes, as described by Brice (1970). The resulting electromagnetic wave-particle interaction would scatter resonant electrons down the field line into the atmosphere. One reason for this emphasis is simply due to the large amount of published work concerning cyclotron instabilities driven by magnetospheric particles (Kennel and Petschek, 1966; Brice, 1970; Cornwall, 1966; Cocke and Cornwall, 1967; Kennel, 1969; Cornwall, Coroniti, and Thorne, 1970; Cornwall, Coroniti, and Thorne, 1971; Cornwall, Hilton, and Mizera, 1971; and Brice and Lucas, 1971).

The whistler mode instability involves the cyclotron resonance reaction between ambient magnetospheric particles and electromagnetic waves propagating in the whistler mode.

From the work of Kennel and Petschek (1966), it is found that:

(1) Whistler mode emission is unstable (i.e., wave amplification occurs) when the particle pitch-angle anisotropy, A, exceeds a critical value

$$A > A_c \equiv \frac{1}{\frac{|\Omega|}{\omega} - 1} \tag{1}$$

where Ω is the cyclotron frequency and ω is the wave frequency.

(2) The magnitude of the wave growth rate depends not only on A, but also on the fraction of particles that are resonant. This sets an upper limit to the stably trapped resonant flux which may be expressed as

$$J_{max} = KL^{-4} \tag{2}$$

where L is the L parameter (McIlwain, 1961). Evaluations of K using available electron and proton data (Kennel and Petschek, 1966; Cornwall, Coroniti, and Thorne, 1970; Cornwall, Hilton, and Mizera, 1971; Cornwall, 1968; and Russell and Thorne, 1970) yield a range of $2(10)^9 \lesssim K \lesssim 5(10)^{10} cm^{-2} sec^{-1}$. For discussion purposes we shall use a value of $K \sim 10^{10}$ $cm^{-2} sec^{-1}$.

(3) The resonant particles participating in this interaction must have parallel energy, E, exceeding a critical value

$$E > E_R = \frac{B^2}{8\pi N} \begin{cases} \left(\frac{\Omega_e}{\omega}\right)\left(1 - \frac{\omega}{\Omega_e}\right)^3 & \text{electrons} \\ \left(\frac{\Omega_p}{\omega}\right)^2\left(1 - \frac{\omega}{\Omega_p}\right)^3 & \text{protons} \end{cases} \tag{3}$$

where B is the magnetic field strength and N is the ambient plasma density. Using the critical

pitch-angle anisotropy, A_c, we have for the resonant particles

$$E_R = \frac{B^2}{8\pi N} \begin{cases} A_c^{-1}(1 + A_c)^{-2} & \text{electrons} \\ A_c^{-2}(1 + A_c)^{-1} & \text{protons} \end{cases} \quad (4)$$

From the above, it can be seen that an ambient trapped particle population exceeding both the critical pitch-angle anisotropy, A_c, and the critical intensity above the resonant energy, $J_{max}(E > E_R)$, will stimulate an exponential growth rate for electromagnetic waves propagating in the whistler mode through that particle distribution. The amplified waves will in turn interact with the ambient particles (with $E > E_R$) and scatter then down the field line into the atmosphere. In this way the pitch-angle distribution proceeds towards isotropy, the intensities are lowered to or below the critical intensity, the wave growth is attenuated and the turbulence stops. Note that no limit due to whistler mode turbulence is placed on particle intensities at energies below the resonant energy.

From (4), it is seen that as the ambient plasma density is increased, the resonant particle energy is lowered. Thus particles at the new lower resonant energy become subject to the stable trapping limit and, if the ambient energetic particle spectrum is soft, large intensities of the newly resonant particles will be precipitated into the atmosphere. This has been pointed out by Brice (1970) who also noted that results from synchronous altitude (McIlwain, 1970) showed a relative lack of $\leq$ few hundred eV particles near local midnight, making this region a most suitable candidate for the artificial precipitation of energetic particles--low, cold plasma density plus soft energetic particle spectrum.

The following discussion will illustrate in a semi-quantitative way some of the expected effects of cold plasma injection at geostationary altitudes. The numbers used are "typical" values observed and should be considered as guideline values only. It is clear that to optimize expected results (i.e., maximize the precipitation intensity) the characteristics of the ambient environment in the geostationary injection region must be monitored in real time in order to pick the most suitable conditions for triggering instabilities.

2.1 Electrons

Values for A range from ~ 1/6 to ~ 1. We shall use $A_c \simeq 1/2$ for illustrative purposes. Using this value yields for the electron resonant energy

$$E_R = \frac{B^2}{9\pi N} \simeq 2.1(10)^6 N^{-1} L^{-6} \text{ keV}$$

and at L = 6.6 earth radii

$$E_R = 25N^{-1} \text{ keV}$$

Thus 25 keV electrons are precipitated at an ambient plasma density of 1 cm^{-3} provided intensities exceed $J_{max}(E > 25 \text{ keV})$. Since N ~ 1 cm^{-3}, is a typically observed density in the high-altitude outer-zone region, strong precipitation of tens of kilovolt electrons should be seen under naturally occurring magnetospheric conditions. In fact, Kennel and Petschek (1966) use the observation that outer-zone trapped electron fluxes > 40 keV are usually at or just below the critical intensity as an argument for the occurrence of the whistler mode instability. Furthermore, the occurrence of strong pitch-angle diffusion, identified by the observation of electron intensities isotropic through the loss cone at high latitudes and low altitudes, is a characteristic feature of the outer magnetosphere (Williams, 1970, and Fritz, 1968).

We thus see that, as the ambient plasma density is increased, larger and larger fluxes of trapped electrons (at the new, lower resonant energies) will participate in the whistler mode instability and be precipitated into the atmosphere. For example, at a density of 10 cm^{-3}, the resonant energy becomes $E_R \sim 2.5$ keV. Using a flux of electrons greater than 2.5 keV of 10^9 - 10^{10} $cm^{-2}sec^{-1}$, this represents an available energy flow of 3.8-38 ergs $cm^{-2}sec^{-1}$. The amount per unit time at the equator available to the ionosphere is given in the strong diffusion limit as the ratio of the loss cone solid angle to 2π, times the available energy flow on the field line. Using normal variations in B at geostationary altitudes, the above example yields an energy flow of 0.03 - 0.30 ergs $cm^{-2}sec^{-1}$ (30-300 $\mu W\ m^{-2}$) available to the ionosphere per unit flux tube at the equator.

Thus, by choosing suitable injection times by carefully monitoring the ambient environment (particles and fields), it appears possible to create significant energy flows in the magnetosphere by triggering the whistler mode instability at geostationary altitudes through the injection of cold plasma in a density range of somewhat less than 1 cm^{-3} to a few tens cm^{-3}. Energy is carried to the atmosphere by the precipitation of previously stable trapped electrons. The energy deposition in the atmosphere will be governed by the equatorial area affected by the injection process.

2.2 Protons

Equation (4) (protons) holds when the ambient ions are protons. We are proposing to inject a plasma consisting of heavy ion (barium and cesium)-electron pairs. Cornwall (personal communication) shows that the addition of heavy ions increases the wave speed which, in turn, raises the proton resonant energy. This has the effect of stabilizing the

proton population. Note that this result relates specifically to the whistler mode instability and assumes no other turbulent modes are triggered which would affect the protons. Since the accuracy of this assumption is unknown, we will conduct a parallel theoretical effort aimed at improving our knowledge of other potential magnetospheric instabilities.

The above discussion points out the usefulness of developing the capability of a light-ion plasma injection, such as hydrogen, for future flights. The discussion for electrons then applies to protons with ambient densities of ~ 3 to 10 cm^{-3} being able to precipitate most to all of the ring-current protons. This would represent a significant advance, as protons represent the largest particle energy density available in the magnetosphere.

3. ARC-1 Program

We propose using a satellite, ARC-1, to inject cold plasma into the ambient space environment at geostationary altitudes. As a result of this cold plasma injection, plasma instabilities will be triggered which will scatter the ambient charged particle population down magnetic field lines into the atmosphere. Presently available materials for cold plasma injection (barium, cesium) will set up pitch angle diffusion processes affecting primarily the energetic ($\gtrsim$ few keV) electron population. The magnitude of the resulting ionospheric disturbances will depend on the nature of the instability triggered and on the intensity of the ambient trapped population at satellite altitude, but should be well within the observational capabilities of existing ground instrumentation. The stimulation of visible aurora and/or magnetic substorms is also possible.

A summary of the satellite program, the data handling program and the ground support are presented in this section.

3.1 Satellite Program, ARC-1

A satellite is one of the most cost-effective means to accurately perform the space environment modification studies proposed herein. The satellite platform, in conjunction with a ground support and real-time data handling program, affords:

(1) Injection of cold plasma over wide dynamic range of densities (several orders of magnitude).

(2) Multiple injections.

(3) Optimal injection times through on-board monitoring of ambient environment.

(4) Ability to choose location of injection region to coincide magnetically with the location of ground support instrumentation.

(5) Accurate measurement of cause-effect relationships.

Having decided on a satellite as our experiment platform, it remains to define and describe its details. A preferred configuration is described, ARC-1, with several modifications shown where weight and cost trade-offs can be made. The primary experiment is the plasma injection package and the support experiments are the particle and field instruments necessary for observing the queiscent and perturbed ambient environment.

Table 1, 2, and 3 show respectively, general ARC-1 characteristics, an overall weight breakdown for ARC-1 and three alternative configurations, and a more detailed subsystem description for ARC-1 and two alternative configurations. The ion source configuration shown for reference in table 2 is not included in table 3, as this particular configuration is not considered suitable for the initial launch. Figures 2, 3, and 4 shown more details of ARC-1 and its internal configuration.

The tables show that as total weight is reduced:

(1) Additional cost may be incurred.

(2) Total injection yield is reduced.

(3) Support experiments are compromised.

(4) A shelf-life and reliability problem appears in the battery area.

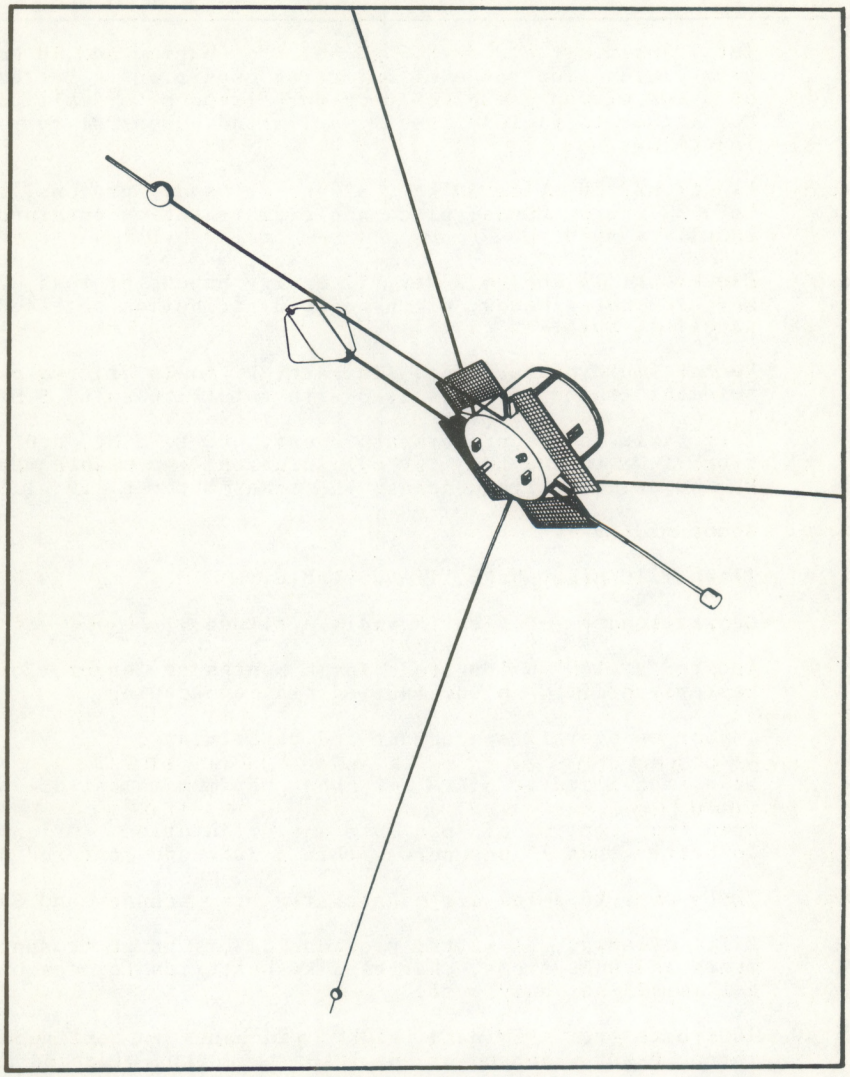

Figure 2. ARC-1 spacecraft. Electric field booms, VLF loop antennae, fluxgate magnetometer boom, and solar cells are clearly visible.

With the above points in mind, it is to be realized that all configurations shown will provide a meaningful experiment, with the preferred configuration being ARC-1.

Table 1. ARC-1 Characteristics

Plasma injection:	Total ionized yield of 8.5 gm moles of barium and 40 gm moles of cesium yields wide range of injection conditions. Battery cycle life of ≈ 100 discharges gives necessary freedom for multiple injections. Hot filaments yield virtually unlimited number of very low intensity injections.
Low-energy particle measurement:	Electrons, 10 eV to 30 keV, 32 energy bands; protons, 10 eV to 30 keV, 32 energy bands; pitch-angle distribution obtained by utilizing satellite spin.
High-energy particle measurement:	Electrons, 15 keV to 2 MeV, 17 energy bands; protons, 20 keV to 8.5 MeV, 10 energy bands; pitch-angle distribution obtained by utilizing satellite spin.
Magnetic field:	Vector field measurement, fluxgate, DC to 10 Hz; two axis loop measurement (third axis resolved with satellite spin) 3 Hz to 200 kHz.
E-field:	Three axis double probe measurement.. DC to 3 Hz, 0.01 mV/m resolution; 1 Hz to 200 kHz, 1μV/m resolution; impendance measurement at DC and selected frequencies; VLF transmitter @ 1.0, 1.5 and 3.3 kHz.
Suggested launch date:	About mid-1974.
Launch vehicle:	Titan IIIC piggy-back, if available.
Orbit:	Geostationary (~6.6 earth radii altitude).
Stationkeeping:	Located at 169° W longitude for 6 months or longer, followed by Easterly drift. No inclination station keeping.
Lifetime goal:	1 year on overall spacecraft and experiments.
Stabilization:	Spin stabilized at 6 RPM ±1% about maximum moment-of-inertia axis.
Attitude control:	Open loop control of spin rate and orientation. Orientation control to better than 1° anywhere within a 30° cone centered on Sun.
Aspect determination:	Three axes to a few arc minutes via star scanner and Sun sensors.
Power capability:	8 ft^2 of array, 71 watts, provides 24-hr. power to support instruments and subsystems; charges 2 kw batteries for cesium injection on a 10-min/3-day duty cycle.
Telemetry data:	4096 bits sec^{-1} PCM data (+10kHz wideband) in continuous mode; three 10-kHz wideband or one 10kHz to 200kHz wideband analog channels for ±2 hours about suborbital midnight.
Thermal:	All passive temperature control, -10 to +30°C internal temperature.
Size:	3 feet in diameter by 2 feet high, with two 6-foot booms and four 20-foot booms. Launch envelope ≈ 5' x 5' x 3'.
Weight:	About 350 pounds, including 175 pounds of primary and support experiments. Several modifications available.

Table 2. Weight Breakdowns

	ARC-1	Mod 1	Mod 2	Ion Source
Prime experiment--plasma source	70.0 lbs.	50.0 lbs.	40.0 lbs	20.0 lbs.
Batteries	56.0	56.0	12.0	89.0
Support experiment--electric field	16.0	5.3	5.3	5.3
Support experiment--high-energy particles	7.0	7.0	7.0	7.0
Support experiment--low-energy particles	10.5	10.5	5.5	5.5
Support experiment--magnetic field	11.9	11.9	11.9	11.9
(Total, experiments, including 5.0 lbs. miscellaneous)	176.4 lbs.	140.7 lbs.	86.7 lbs.	143.7 lbs.
Structure and temp control subsystem	50.5	37.5	32.6	37.5
Elec power subsystem (Less Exp. Batteries)	28.4	24.0	23.2	24.4
Control subsystem	66.5	29.9	29.0	29.9
T&C subsystem	25.5	25.5	25.5	25.5
Ballast	8.0	6.0	3.0	6.0
TOTALS	355.3 lbs.	263.6 lbs.	200.0 lbs.	267.0 lbs.

Table 3. Subsystem Descriptions

	ARC-1	MOD 1	MOD 2
Prime Experiment			
Plasma source	Hybrid	Hybrid	Hybrid
Weight			
Barium	50 lbs.	35 lbs.	30 lbs.
Cesium Vaporizer	20 lbs.	15. lbs.	10 lbs.
Total Ionized Yield			
Barium	8.5 gm moles	6 gm moles	5 gm moles
Cesium Vaporizer	40 gm moles	25 gm moles	15 gm moles
Batteries	AgCd	AgCd	AgZn
Weight	56 lbs.	56 lbs.	12 lbs.
Output	2 kw for 10 min	2 kw for 10 min	1 kw for 5 min
Shelf life	~ 2 years	~ 2 years	~ 6 months
Cycle life	~ 100 discharges	~ 100 discharges	~ 5-10 discharges
Test program required?	No	No	Yes
Support Experiments			
E-field	2 sets of retractable booms - 20' each boom	1 set non-retractable booms	1 set non-retractable booms
Weight	16 lbs.	5 lbs.	5 lbs.
Low-energy particles	Electrons, protons, 10 ev - 30 kev, 32 energy bands each	Electrons, protons, 10 ev - 30 kev, 32 energy bands each	Electrons, protons, 10 ev - 20 kev, 16 energy bands each
Weight	11 lbs.	11 lbs.	6 lbs.
Spacecraft Subsystems			
Weight	53 lbs.	16 lbs.	16 lbs.
Propulsion	N_2 ($45K)	Hydrazine ($300-400K)	Hydrazine ($300-400K)
Structure	51 lbs.	38 lbs.	33 lbs.
	2' x 3'	2' x 2'	2' x 2'

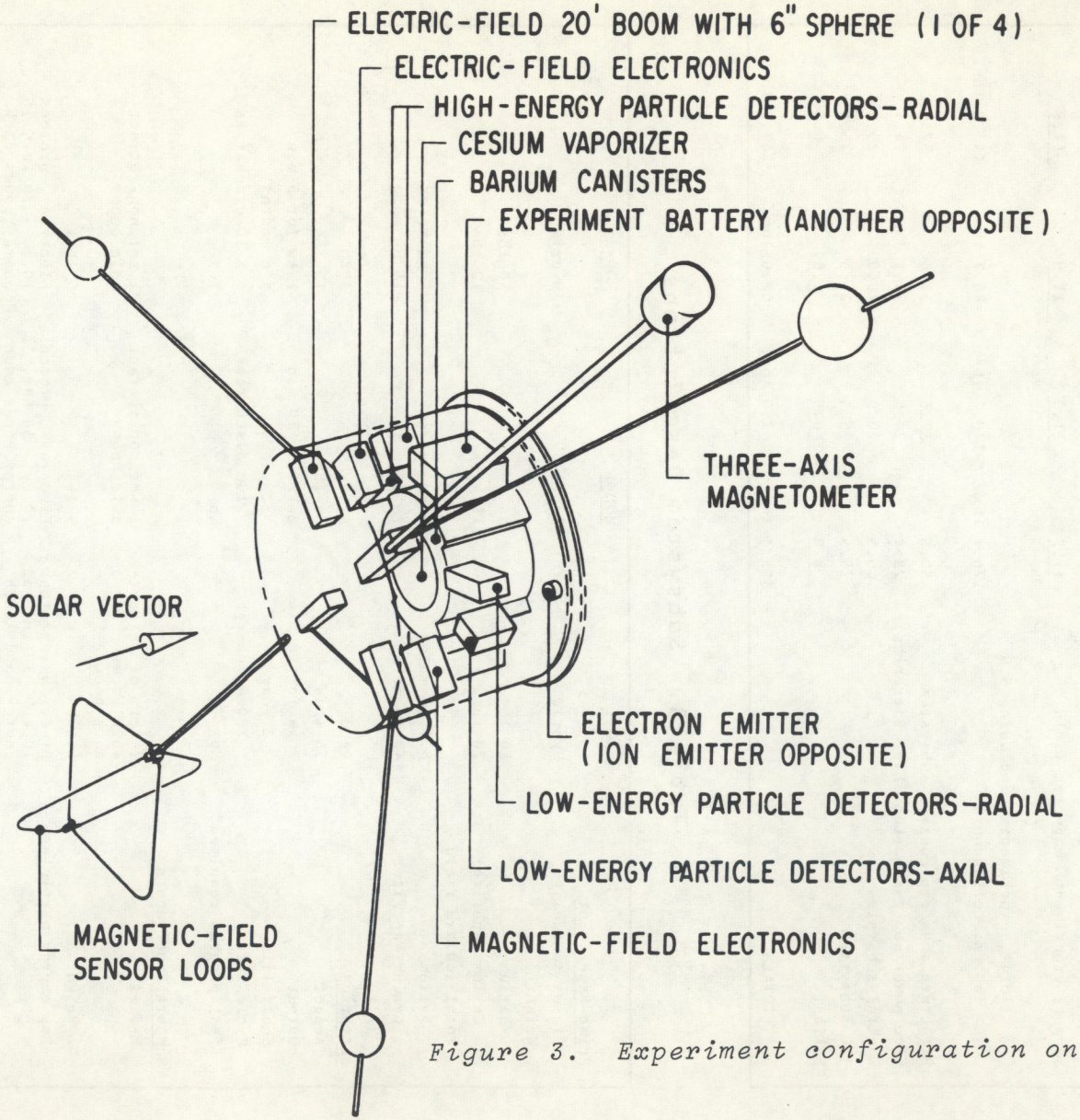

Figure 3. Experiment configuration on ARC-1.

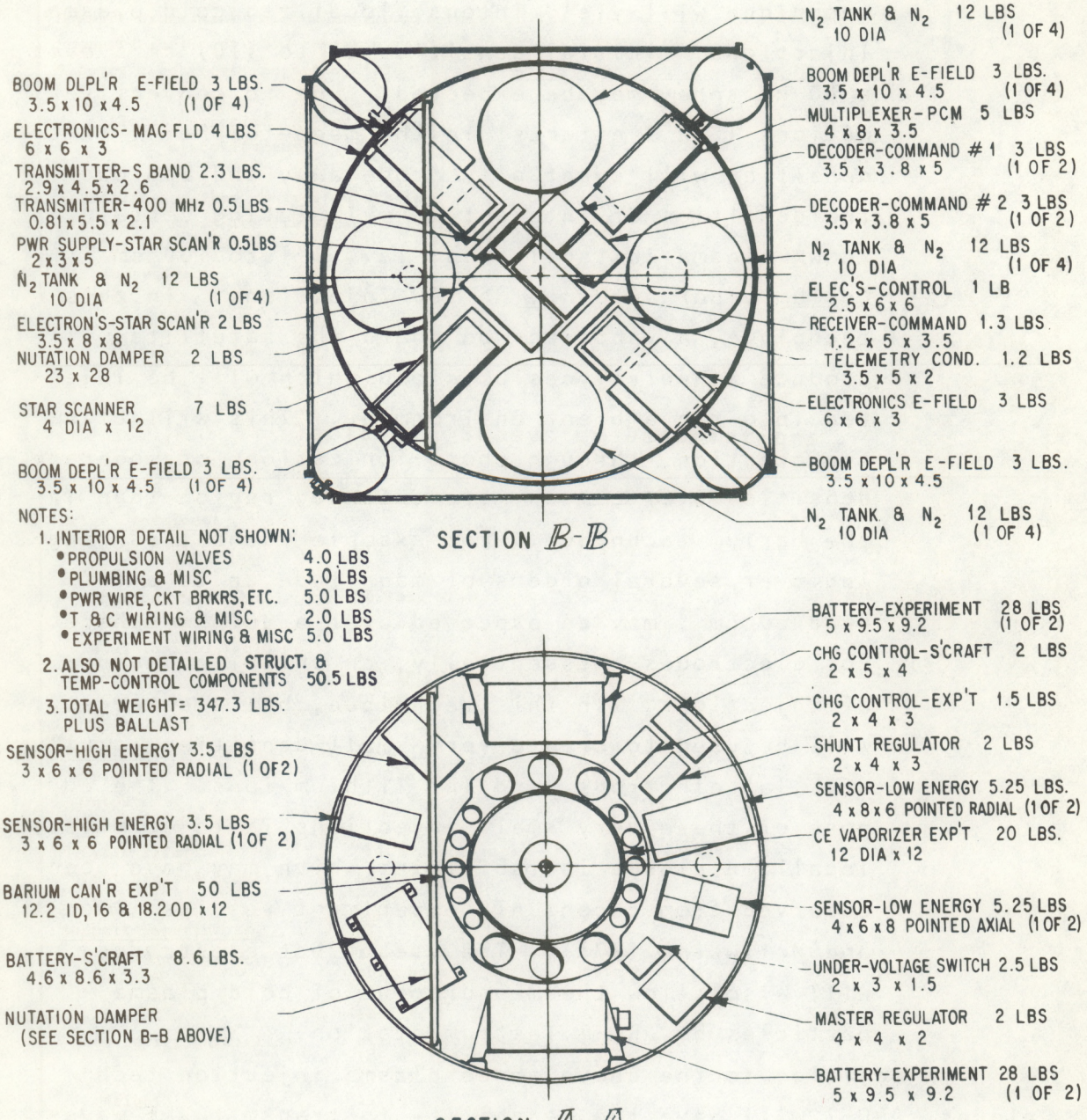

Figure 4. Detail of internal configuration of ARC-1.

ARC-1 incorporates the capability of multiple injections from three methods of cold plasma injection:

(1) Barium canister release. Several injections. This technique will yield intense localized cold plasma injections. Initial densities up to $(10)^4 cm^{-3}$ over a 40-km sphere may be expected. Due to convective motions ($\bar{E} \times \bar{B}$ effects) in the magnetosphere, these densities will eventually erode away and approach the densities of interest in stimulating certain known plasma instabilities; i.e., ~ 1 to 100 cm^{-3}.

(2) Cesium vapor seeding. $\geq$ 100 injections. In this technique, a vaporizer on board the satellite will produce a neutral cesium cloud which will be injected into the ambient environment. This will allow the creation, through photo-ionization, of moderate densities over a much more extended region than in the barium technique. For example, densities ranging over several orders of magnitude up to a few hundred cm^{-3} may be expected over a 300-km sphere.

(3) Hot electrodes. Essentially, an unlimited number of injections. In this technique, hot electrodes will be used to create very small densities locally of: (a) electrons; and (b) lithium ions. The purpose of these very small injections is to stimulate localized plasma instabilities which may have been observed from recent ATS experiment results (DeForest and McIlwain, 1971). The use of hot electrodes will also allow the measurement of cold plasma particles by ARC-1 instrumentation.

In addition to the above three plasma injection techniques, ARC-1 will have the capability to transmit VLF waves into the ambient medium in a further attempt to precipitate trapped particle fluxes.

All necessary instrumentation required for monitoring the state of the ambient plasma will be included aboard the satellite. This instrumentation consists of electron and proton intensity observations from 10 eV to several MeV in energy, DC and AC magnetic fields, and DC and AC electric fields and is summarized in table 4. This instrumentation will be used to choose the optimum time for plasma injection, as well as to measure the response of the ambient plasma during and after injection.

3.2 Data Handling Program

The data handling aspects of the ARC-1 experiment consists of three phases, each designed to optimize the scientific and technical results of the program. These are:

(1) Reception and reduction of the ARC-1 data will be accomplished at the Space Environment Laboratory (SEL) real-time data reception facility located on Table Mountain in Boulder, Colorado. Data will be received and displayed in real time in order to select injection times, and will be recorded on magnetic tape for research and analysis purposes. Data from both ARC-1 and the ground support program will be utilized in real time. This is shown schematically in figure 5. This type of real-time data system is now in operation in SEL in conjunction with other laboratory programs.

(2) Analysis and interpretation of the data will be accomplished on a time scale which allows input into remaining ARC-1 plasma injections. Quantitative studies of specific instabilities, along with accurate cause-effect relationships, will result from analysis of the entire experiment. The usefulness, potential results, and characteristics of a follow-on program may then be defined.

Table 4. Support Instrument Performance Summary

Instrument	Low-energy Particles	High-energy Particles	VLF, ELF E-& B-Fields	DC E-Fields	DC Mag Field
Weight (lbs)	11	7	4*		5*
Power (watts)	4.5	2	4.25		4
Sensitivity Range	Electrons & protons: 10 eV-30 keV in 32 steps, 18° pitch-angle resolution	Electrons: 15 keV-2 MeV in 17 steps. protons: 20 keV-8.5 MeV in 10 steps. 12.5° pitch-angle resolution	E: 1 Hz-200 kHz 1 μV/m resolution three axes; B: 3Hz-200 kHz, 28" square loops, two axes; E-field impedance meas, E-field xmtr	DC-3 Hz 0.01 mV/m resolution, 3 axes	DC-10 Hz 3-axis flux-gate
Telemetry (words/sec)	192	22.4	43.5	32	144

*Booms, VLF loops, and boom drive hardware add 18.9 lbs to the total weights of the fields instruments.

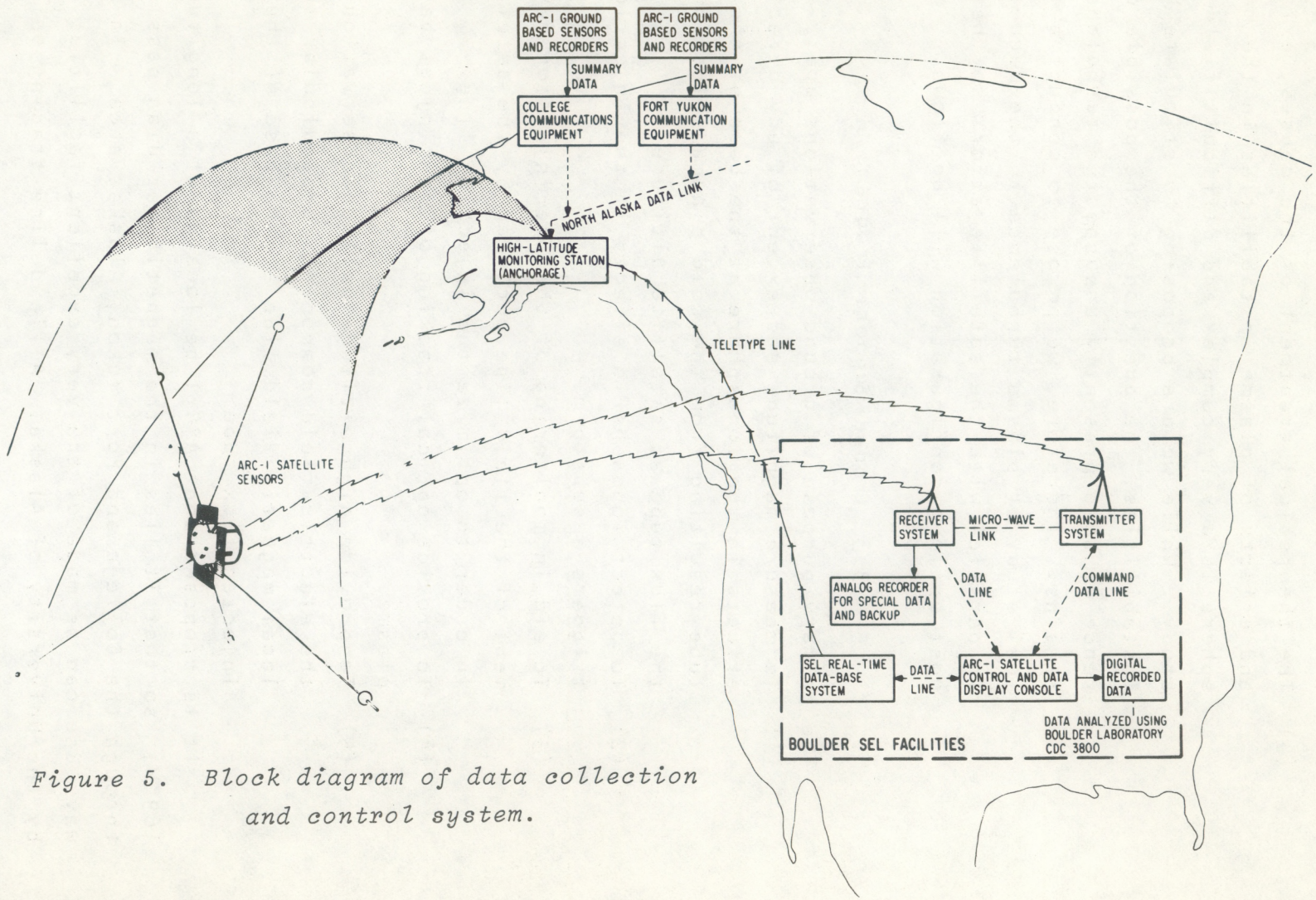

Figure 5. Block diagram of data collection and control system.

(3) The theoretical treatment of the causes, existence, and effects of plasma instabilities in the magnetosphere is a very complex and difficult field of study. While we are proposing to stimulate known instabilities, the question of the possible occurrence of some presently unsuspected turbulence remains. Therefore, we propose to conduct a theoretical study of plasma turbulence in the magnetosphere in parallel with the satellite effort so that the most optimum configuration will be flown.

3.3 Ground Support Program

The primary purpose of ground observations are:

(1) To measure magnitude and extent of any direct effects in the ionosphere at the base of the flux tube resulting from the cold plasma injection in the flux tube at satellite altitude.

(2) To detect ionospheric effects if the injection triggers a substorm.

(3) To aid in monitoring of the pre-injection environment of the field line occupied by the satellite in order to optimize the injection line.

(4) To provide optical tracking of the inject barium plasma.

(5) To provide high altitude balloon observations of the electric field component perpendicular to the local magnetic field line at the base of the injected flux tube.

It is proposed that ARC-1 be located at a longitude of 169°W, so that it lies in the magnetic meridian passing through the College and Fort Yukon, Alaska, area. In this way, use can be made of the very excellent facilities offered by the University of Alaska. A field line tracing on the

computer using the 1962 Jensen and Cain field expansion shows that the foot of the injected flux tube (100-km altitude) is in the Fort Yukon area (see fig. 6). Because of the necessity to detect effects covering a wide dynamic range in intensity, as well as effects covering a wide spatial extent (due to flux tube displacements as large as approximately 100 km), the following observing program is proposed as the primary ground observing program in the Fort Yukon-College area:

(1) All sky cameras.
(2) Magnetometers.
(3) Visual observers.
(4) Image orthicon televisons.
(5) Pointed photometers.
(6) Merdian scanning photometers.
(7) Coherent 50 MHz radar.

This program is heavily weighted toward detection of optical effects, mainly because observation of these effects allows the greatest dynamic range in detection, the best signal-to-background noise and the best means to obtain quantitative information about any particle precipitation triggered by the cold plasma injection experiments. Other observations of a desirable nature can also be performed at relatively low cost utilizing instrumentation already available through other programs. Two examples are riometers on the College-Fort Yukon meridian jointly operated by NOAA and the Geophysical Institute, and the incoherent scatter radar at Poker Flat jointly operated by SRI and the Geophysical Institute.

It is also proposed that during injection times a high-altitude-balloon program be conducted which yields measurements of the electric field component perpendicular to the magnetic field line at the base of the flux tube injected. Such flights lasting several hours will yield invaluable information concerning characteristic electric field behavior

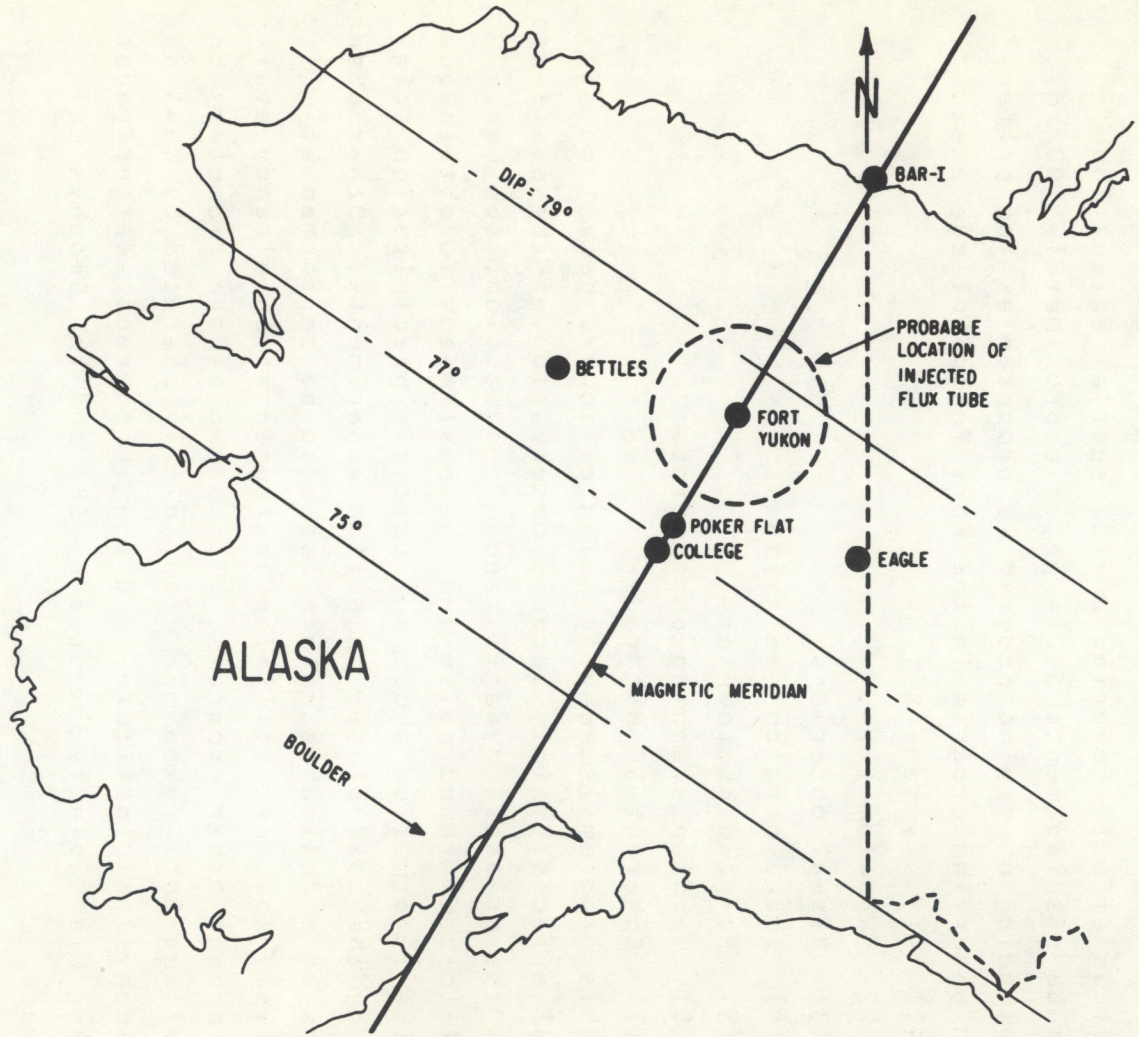

Figure 6. Intersection of injected flux tube with upper atmosphere.

at the onset of a magnetic substorm. These data will be valuable in determining optimum injection times.

Instrumentation existing at several observatories both in the North and South American continents can be used to visibly track the barium ion clouds formed. Such observations will be very useful in determining the ultimate size of the cloud, as well as for diagnosing the motion of the injected material. Sites are operated by both the National Aeronautics and Space Administration and the Max Planck Institute of the West German Republic.

4. EXPECTED RESULTS

If, as expected, the injection of cold plasma at geostationary altitudes is capable of establishing conditions necessary for triggering the whistler mode instability, what magnitudes are expected for the resulting electron precipitation events? Over what areas do we expect observable effects? How do these results compare with earlier predictions? In this section, we present a discussion of and initial answers to these questions.

4.1 Precipitation Intensities

We illustrate the concept of using cold plasma injection to trigger the whistler mode instability in figure 7. All the data pertain to geostationary altitudes (6.6 earth radii).

The top portion of figure 6 shows a plot of the resonant energy, E_R, as a function of density (4) for electrons with $A_c = 1/2$. The band of values shown allows a ± 50 percent variation in the ambient magnetic field.

The lower portion of figure 7 shows both a plot of the integral omnidirectional electron flux and the corresponding energy flux as a function of electron energy. The limiting flux (2) is shown for $K = 10^{10} cm^{-2} sec^{-1}$. The shaded region

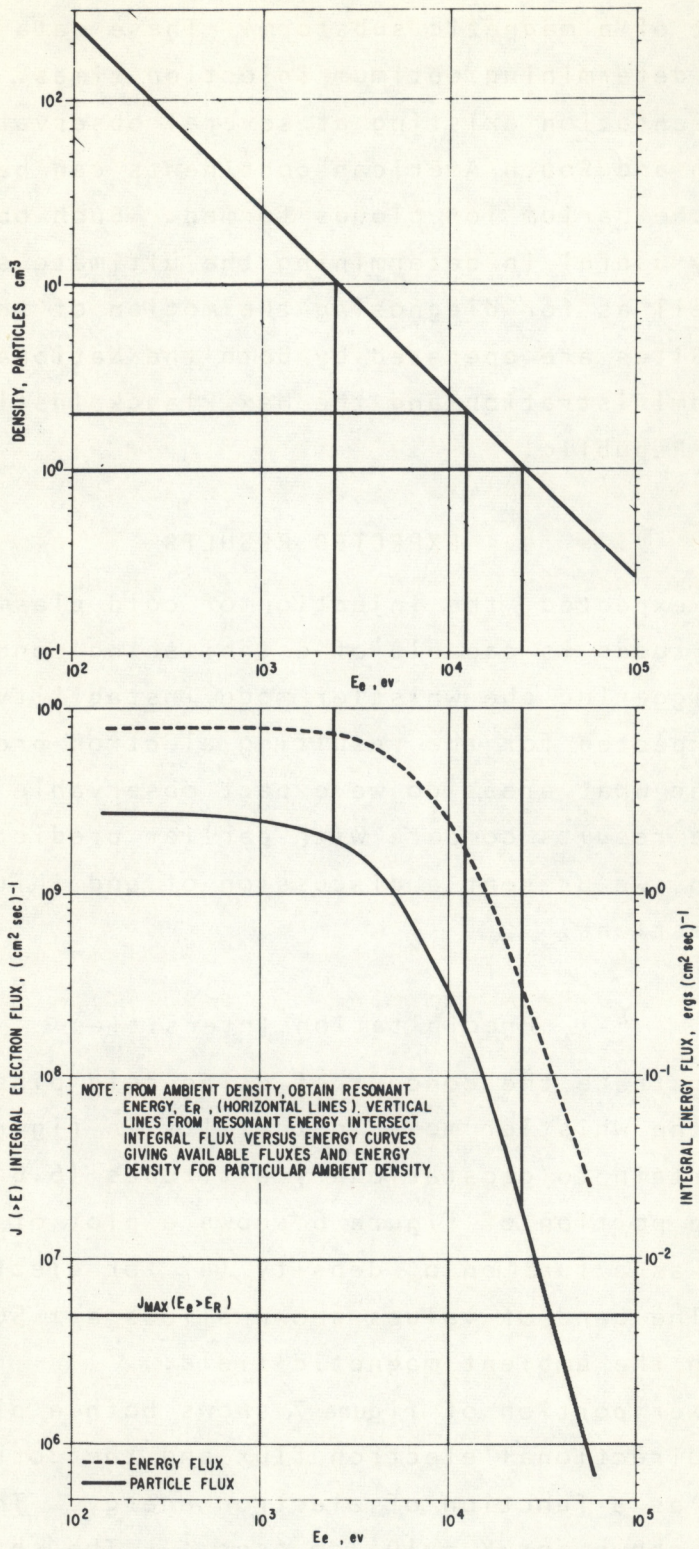

Figure 7. Example of particle fluxes available for whistler mode instability.

allows for an uncertainty of a factor of ten in the limiting flux. The integrated flux in figure 7 yields an ambient density of 1 cm^{-3}.

At ambient density of 1 cm^{-3}, electrons of energy $E_R >$ 25 keV are just beginning to stimulate wave growth and initiating a strong precipitation event. Figure 7 shows that increasing numbers of newly resonant particles participate in the instability resulting in an intense precipitation event with significant energy flow. In the strong diffusion limit the maximum energy flow at the equator available to the ionosphere due to the absolute spectrum in figure 7 is $\sim$ 0.08 ergs $cm^{-2}sec^{-1}$ (80 $\mu W\ m^{-2}$). We shall see that equatorial areas up to $\sim 7(10)^4 km^2$ can be affected yielding an energy flow to the ionosphere of $5.6(10)^{13}$ ergs/sec ($5.6(10)^6$ watts). The affected ionospheric area of $\sim$ 200 km^2 receives an energy deposition of $\sim$ 28 ergs/cm^2sec ($2.8(10)^4 \mu W/m^2$).

Energy distributions very similar to that shown in figure 7 have been observed in the nightside hemisphere during a two day sampling period at geostationary altitude (DeForest and McIlwain, 1971). Intensity variations indicate that in the strong pitch angle diffusion limit (assuming no feedback from the ionosphere), the maximum energy deposition rate to be expected from triggering the whistler mode instability is a few hundred ergs $cm^{-2}sec^{-1}$ (10^5-10^6 $\mu W\ m^{-2}$). By contrast, the lower limit for ground instrumentation sensitivities is $\sim$ 0.1 ergs $cm^{-2}sec^{-1}$ and visual observation is possible when $\gtrsim$ 1 to 2 ergs $cm^{-2}sec^{-1}$ are deposited in the lower ionosphere. Note that although the growth rate, γ, depends on the fraction of resonant particles and therefore inversely on the density, the integrated growth along the field line,

$$\Gamma = \int \frac{\gamma ds}{v_G}$$

where v_G is the wave group velocity, turns out to be independent of density. The reason is that the wave group velocity is also inversely proportional to the density. Therefore, although the differential growth rate, γ, decreases as N increases, the waves slow down and spend more time in the amplification region. This yields an integrated growth, Γ, which depends only on the number of resonant particles.

We emphasize that the above values are guidelines for what can reasonably be expected from a "triggered" event. Observed intensities and spectra at geostationary altitudes vary over wide limits. In addition, the available estimates of key parameters, such as the critical flux, are quite uncertain. We are attempting to overcome these problems in three ways:

(1) Support instruments will monitor the environment in real time to optimize the injection time.

(2) Plasma injection will allow multiple injections covering ranges in density of several orders of magnitude.

(3) A continuing theoretical effort concerning magnetospheric plasma instabilities will be supported.

With the above in mind, the preceding discussion does indicate the high feasibility of significant power flow initiated by artifically triggered whistler mode turbulence.

4.2 Precipitation Region

4.2.1 Barium Release

This cold plasma injection technique yields very large initial densities and has been used often in the past, primarily for studying electric fields above the atmosphere. We have chosen this technique as one of our injection modes because it is a proven method of establishing high cold plasma densities in a localized region. Several releases are

planned yielding an injection range of 0.1 to 5 gm moles of fully ionized barium.

The satellite position will be near the edge of the barium cloud in order to:

(1) Observe particle/field response near region of high plasma density gradient.

(2) Avoid coating the satellite with barium ions.

To estimate the spatial size of the affected region, let us consider, for example, the release of 1 gm mole [$6(10)^{23}$ ion-electron pairs] of fully ionized barium. Approximately 20 seconds after exploding the canister, the available barium vapor has been fully ionized and the ion cloud expands across field lines until

$$\frac{B^2}{8\pi} = \text{kinetic energy density of the cloud}$$

Using B = 100 γ as a representative field at geostationary altitudes and a thermal velocity for the barium of 1.2 km sec^{-1} (1 eV) gives

$$\frac{B^2}{8\pi} \sim 4(10)^{-8} \text{ ergs cm}^{-3} = \frac{6(10)^{23} \text{ eV} \times 1.6(10)^{-12} \text{ ergs}}{4/3\ \pi\ r^3}$$

from which r $\sim$ 20 km.

Therefore, during the 20-second expansion of the neutral cloud while ionization is taking place, a number density is reached where expansion of the newly created ion cloud normal to the field is halted. A bubble of ionized barium exists into which the ambient magnetic field is unable to penetrate. The density at this time, $\sim$ 20 seconds after canister explosion, is $\sim 4(10)^4 cm^{-3}$. Assuming the ion cloud continues to expand along the field line at its thermal velocity, the density will drop to $\sim 4(10)^3 cm^{-3}$ in 10 minutes. In addition, during the time when the ambient magnetic field is excluded from the plasma bubble, the edges of the bubble are eroded away due to the action of the $\overline{E} \times \overline{B}$ force. Thus the ambient magnetic field is able to return toward its pre-injection condition in several minutes.

Densities in the range of interest will be attained within 10 to 20 minutes after the explosive release of the barium. At this time the ambient magnetic field and its particle population will permeate the ion cloud. A minimum radial extent at the equator should be $\sim$ 20 km.

This area of $\sim 10^3 km^2$ at the equator projects to an area of $\sim 3\ km^2$ at the top of the atmosphere. Thus, a very localized disturbance is expected for these conditions, so that a wide field of view is required in the ground support instrumentation.

4.2.2 Cesium Vaporization

This technique has the advantage of injecting moderate densities over a much larger region of the magnetosphere. The injection rate of cesium atoms will be varied over several orders of magnitude up to a maximum of 10^{22} atoms sec^{-1}. We shall use this rate for discussion purposes, realizing that resulting densities can be varied downwards many orders of magnitude.

Relevant parameters are:

Cesium photo-ionization e-folding time$\simeq$18 min $\sim$ 1000 sec

Cesium atom thermal velocity $\simeq$ 0.3 km sec^{-1}

ARC-1 orbital velocity $\simeq$ 3.2 km sec^{-1}

Since the orbital velocity is much larger than the cesium atom's thermal velocity, a reasonable approximation is that the cesium vapor moves tangentially with the satellite while slowly expanding along the radius vector. To obtain a rough estimate of the density, we shall assume spherical expansion as the vapor moves radially away from the spacecraft.

In one e-folding time, the cesium will have traveled 300 km. Assuming roughly spherical expansion during this time yields a volume of $\sim 1.4(10)^7 km^3$. Using the maximum injection rate of 10^{22} atoms sec^{-1}, injection periods ranging from 0.5 to 10 minutes will yield densities from $\sim$ 10 to

300 cm^{-3}, with several orders of magnitude smaller densities available from lower injection rates.

In the above approximation, the flux tube equatorial area affected is $\sim 7\ (10)^4 km^2$. From the corresponding ionospheric area of $\sim 200\ km^2$ and the spectrum in figure 7, a value of $2.8\ (10)^4\ \mu W\ m^{-2}$ can be precipitated into the ionosphere with the above densities. This corresponds to a total energy flow to the ionosphere of $5.8(10)^6$ watts. Note that this energy flow is $\sim$ 100 percent efficient in its ionization capability.

The above area estimates will increase and densities will decrease correspondingly due to $\overline{E} \times \overline{B}$ drift effects. The magnitude and direction of this drift varies greatly and is a principal reason for our attempts to measure the local $\overline{E}$-fields. We note that $\overline{E}$-field values of 0.01 to 1 mV m^{-1} and $\overline{B}$ values of 50 to 150 γ yield drift velocities of from $\sim$ 0.05 to 15 km sec^{-1}. This range of v_{drift} values includes the cesium thermal velocity and the orbital velocity, and will affect the motion of the ion cloud, particularly in the high velocity range. However, the preceding values are useful estimates and indicate the feasibility of sizeable energy dumps into the ionosphere initiated by cold plasma injection techniques at high altitudes.

4.2.3 Hot Electrodes

We expect only very localized disturbances with this technique. It is being used to investigate the possibility of stimulating electrostatic instabilities which, in turn, accelerate a fraction of the ambient low-energy population to high energies. If successful and enough energetic particles are formed, it then becomes feasible to consider the possibility of the new energetic particles violating the stably trapped limit and triggering the whistler mode instability.

The weight, power, and cost of the hot-electrode technique is so small and the potential return so high that we feel it should be flown.

4.2.4 Earlier Injection Estimates

The previous estimates, by Brice (1970) and by Brice and Lucas (1971), of a required 1 kg mole of injected cold plasma were obtained for a much larger scale effect.

For example, Brice (1970) based the 1 kg mold estimate on filling an entire flux tube, with an area of 4000 km^2 at 1000 km altitude, to a density of 15 cm^{-3}. It is only necessary to populate the region near the magnetic equator with cold particles, since this is where most of the wave amplification occurs. By reducing the flux tube diameter at the equator, the appropriate densities near the equator for triggering the whistler mode instability may be obtained with injections << 1 kg mole, as discussed in the previous section.

Brice and Lucas (1971) obtain a 1 kg mole estimate by requiring the depletion of the entire outer zone. The difficulty (weight, power, and unanticipated side effects) of such a large-scale injection is recognized. Therefore, we are proposing a modest pilot program designed to provide quantitative results concerning the artificial triggering of magnetospheric instabilities.

4.3 Coordinated Measurements with Other Satellites

The ground support program and the data handling and processing effort have been described earlier. We wish simply to point out here that full use will be made of any other opportunities for coordinated measurements. For example, the ATS F and G programs are scheduled for launches in the 1974-1975 time period. These satellites will carry a scientific payload for performing measurements of particles and fields, and will be placed in geostationary orbit at longitudes

different than ARC-1. This provides the capability of simultaneous observations at different longitudes during the injection experiment.

We note that SEL has two experiments aboard both ATS F and G and can carry out the arrangements necessary for a coordinated observational effort.

5. REFERENCES

Brice, N. (1970), Artificial enhancement of energetic particle precipitation through cold plasma injection: A technique for seeding substorms?, *J. Geophys. Res.*, 75, 4890-4892.

Brice, N., and C. Lucas (1971), Influence of magnetospheric convection and polar wind on loss of electrons from the outer radiation belt, *J. Geophys. Res.*, 76, 900-908.

Cocke, W. J., and J. M. Cornwall (1967), Theoretical simulation of micropulsations, *J. Geophys. Res.*, 72, 2843.

Cornwall, J. M. (1968), Diffusion processes influenced by conjugate wave phenomena, *Radio Sci.*, 3, 740.

Cornwall, J. M. (1966), Micropulsation and the outer radiation zone, *J. Geophys. Res.*, 71, 2185-2199.

Cornwall, J. M., F. V. Coroniti, and R. M. Thorne (1970), Turbulent loss of ring current protons, *J. Geophys. Res.*, 75, 4699.

Cornwall, J. M., F. V. Coroniti, and R. M. Thorne (1971), A unified theory of SAR arc formation at the plasmapause, *J. Geophys. Res.*, 76.

Cornwall, J. M., H. H. Hilton, and P. Mizera (1971), Observations of precipitating protons in the energy range 2.5 keV - 200 keV, *J. Geophys. Res.*, 76.

DeForest, S. E., and C. E. McIlwain (1971), Plasma clouds in the magnetosphere, *J. Geophys. Res.*, 76, 3587-3611.

Fritz, T. A. (1968), High-latitude outer-zone boundary region for $\geq$ 40 keV electrons during geomagnetically quiet periods, *J. Geophys. Res.*, 73, 7245-7255.

Kennel, C. F. (1969), Consequences of a magnetospheric plasma, in Magnetospheric Physics, eds. D. J. Williams and G. D. Mead, 349-419, Am. Geophys. Union 1969; *Rev. Geophys.* 7, nos. 1 and 2.

Kennel, C. F., and H. E. Petschek (1966), Limit on stably trapped particles, *J. Geophys. Res.*, 71, 1-28.

McIlwain, C. E. (1961), Coordinates for mapping the distribution of magnetically trapped particles, *J. Geophys. Res.*, 66, 3681-3691.

McIlwain, C. E. (1970), Equatorial observations of auroral plasma, paper presented at International Symposium on Solar-Terrestial Physics, Leningrad, USSR, May.

Russell, C. T., and R. M. Thorne (1970), On the structure of the inner magnetosphere, *Cosmic Electrodynamics*, 1, 67.

Williams, D. J., Sources, losses and transport of magnetospherically trapped particles, ESSA TR ERL 180-SDL 16, 103 pages, Aug. 1970; Invited review paper presented at the International Symposium on Solar-Terrestrial Physics, Leningrad, USSR, May 1970, to be published in the proceedings.